The direction of the water force on a rowing blade and its effect on efficiency

University of Queensland, Mechanical Engineering Report No. 2008/03, April 2008

M. N. Macrossan

Center for Hypersonics, School of Engineering, University of Queensland, Australia

---

Previous estimates of the efficiency of rowing have assumed (in the absence of any better data) that the water reaction force on the rowing blade, the 'blade force', acts in a direction normal to the blade chord-line (oar shaft direction). In 1967 Wellicome suggested that there may be a component of the blade force parallel to the chord-line, pointing outwards, which would make the oar more efficient in the early part of the stroke [*Rowing: A Scientific Approach, A Symposium*, (Williams, Scott, eds.), Kaye and Ward Ltd, London, 1967]. The recent steady-flow $\frac{1}{4}$-scale model tests of Caplan and Gardner [*J. Sports Sciences*, 25:643-650, 2007] detected a small such parallel force on the asymmetrical Macon and Big Blade shapes. It is possible that this component of force is actually zero within the experimental error, but if the direction of the blade force is tilted away from normal by the amount shown in the model tests, the efficiency of rowing propulsion may be one or two percent greater than previously estimated. However, those previous estimates of efficiency ignored the effect of oar bending which could reduce the efficiency of rowing by as much as 5%. There are reasons to suspect that the scale model results cannot be used to predict the magnitude or the direction of the force on a full-size oar during rowing: the flow is unsteady, and a crucial non-dimensional parameter, the Froude number, is significantly different in the two cases. It might be possible to detect a forward component of the blade force during rowing by measuring the tension strain such a force would produce in the oar-shaft outboard of the gate/pivot.

CONTENTS

1. INTRODUCTION

Figure 1 shows a schematic view of a two-oared boat being rowed. The water reaction force on the oar-blades when immersed in the water, the 'blade force' B, acts approximately in the horizontal plane. It has a component in the boat forward direction (the 'propulsive component') which opposes the drag forces acting on the boat and its superstructure. The blade makes a complicated path through the water (shown later in Figure 8); it first moves forward and side-ways, then moves backwards about 0.3 m (when the oar-shaft is close to square to the boat, *i.e.* near 'square-off'), before moving forward again.

Mechanical energy flows from the system (into the water) as the hull exerts a forward force on the water (the opposite of the drag force) and as the blade exerts a backward-force on the water (the opposite of the blade force), *i.e.* the drag and blade forces dissipate the energy of the system. If the average boat speed over the cycle is to be maintained, the rower must do work at a rate sufficient to replace the dissipated energy. For a given boat speed there is a certain amount of energy

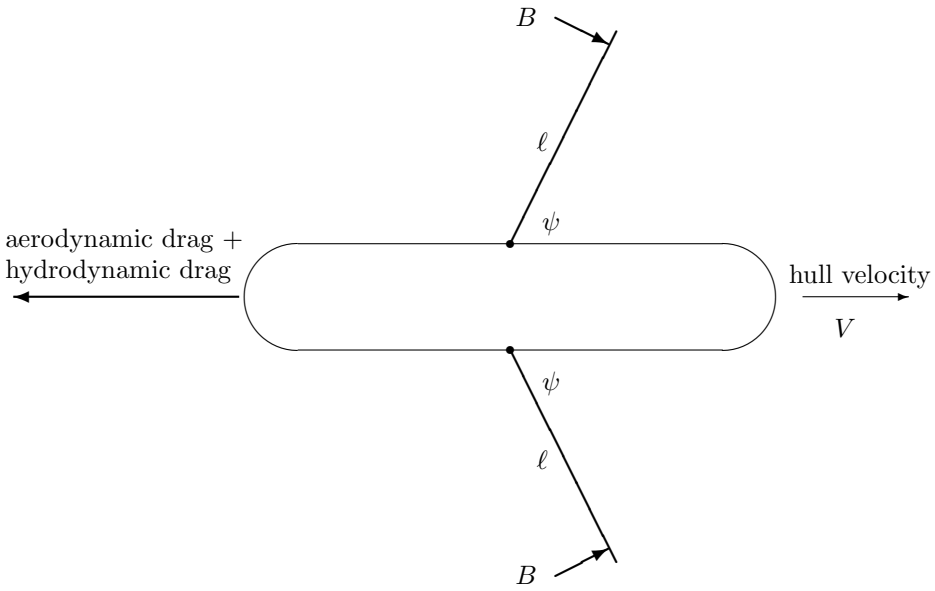

FIG. 1. Schematic of the entire rowing system showing the forces acting on the system: the drag force D and blade forces B acting at a distance ℓ from the oar pivot. The oars make a variable angle ψ to the forward direction. When the oars enter the water (at the 'catch'), ψ is about 40° or less. The moment when $\psi = 90°$ is known as 'square-off'.

extracted/dissipated by the drag forces on the hull and superstructure.[1] The total energy that must be supplied by the rower consists of this 'base load' energy required to move the boat at the desired speed, plus any extra energy extracted from the system by the blade force applied to the water. The less the blade moves in the direction opposite to the direction of the blade force (the less it 'slips'), the less energy that is extracted by the blade force, and the less energy that must be supplied by the rower (for a given boat speed) and the greater the efficiency of the propulsion system.

2. DIRECTION OF THE BLADE FORCE

In the absence of any better data, it is usually assumed [1, 6, 8, 9, 14] that the water reaction force on the blade acts normal to the blade surface (more correctly, since the blade surface is curved, normal to the chord-line of the blade, see Figure 6). It is also usually assumed the blade-chord line is parallel to the axis of the shaft at the gate where the oar angle is measured, *i.e.* that the oar-shaft does not bend significantly when a load is applied. A force acting in this blade-normal direction has a component in the direction parallel and opposite to the velocity of the blade with respect to the water, *i.e.* it has component in the 'blade-drag direction'. This drag component will dissipate energy (extract energy from the system) and detract from the propulsive efficiency of the oar. If the blade force deviated from the normal direction so as to reduce its component in the blade-drag direction the efficiency of the blade would be increased.

Brearley and de Mestre [2] have considered the effect of (a) oar-bending, which decreases the efficiency (see §9) and (b) a beneficial change in the blade force direction away from normal to the oar-shaft axis. For (b), they used some measured data for oar forces and oar angles and assumed the blade force pointed more in the boat-forward direction in the early part of the stroke.[2] There is a gain in forward propulsive force (compared to the force normal case) as the oar sweeps from the 'catch' (where when it first enters the water) to square-off, and a loss of propulsive force after square-off, but a net gain over the entire stroke, since the oar was forward of square-off for most of the stroke. They calculated a gain in propulsive efficiency of 1.7% if the blade force deviated from the normal direction by 5°.

Wellicome [14], in 1967, may have been the first to suggest that the blade force, in some parts of the stroke, might not be normal to the chord-line. Wellicome speculated that

> 'any vortex system close to the tip of the oar would result in considerable force being generated along the edges of the blade so that the total force would not be at right angles to the blade surface. This means that the force on the oar, particularly early in the stroke, will be much more nearly fore and aft (which is what is wanted) than the position of the oar would suggest' (Wellicome [14], p. 24).

The possibility that the resultant force might not be normal to the chord-line seems to have been suggested by analogy with the perfect hydrofoil/airfoil of incompressible, two-dimensional, frictionless (inviscid), rotational flow. For this ideal flow

[1] The energy extracted by the drag forces depends not only on the average boat speed but on the boat speed variation.

[2] They assumed this change in force direction could be produced by a change in the design of the oar, but the effect is similar to a possible change in force direction arising from a hydrodynamic effect on standard oars.

there is a net circulation in the flow around the airfoil (a starting vortex is shed and swept downstream), and this circulation changes the pressure distribution in such a way that the resultant force acts in the direction normal to the velocity of the airfoil relative to the fluid; there is no component of the resultant force in the airfoil-drag direction, and hence the pressure forces dissipate no energy.

Edwards [6] in 1963 wrote that the rowing blade acts 'like the wing of an aeroplane or a hydrofoil'. He noted that the blade is set at an 'angle of incidence' (angle of attack) to its velocity through the water and refers to the force on the blade as the 'lift' when he says[3]

> the 'lift' ... is approximately at right angles to the [chord-line]. (Edwards [6], p. 78.)

If the water reaction force on the blade is normal to the chord line as Edwards assumed, then the superficial similarity of a blade to a hydrofoil is not significant, since a force in this direction has a drag component which dissipates energy. Nolte [13] is a recent and well-known advocate of the idea that the oar blade at the catch acts like a hydrofoil/airfoil.

3. STEADY FLOW, MODEL TESTS

Caplan and Gardner [3] have measured the water reaction force on 1/4-scale models of a 'Big Blade', a Macon blade and a flat 'Big Blade', *i.e.* a plate having the same face-on profile as a Big Blade (see Figure 6) but no curvature of the face which 'pushes' against the water. In a second paper [4] they gave the forces they measured on a rectangular flat plate and two rectangular curved plates. Figure 2 shows the experimental arrangement schematically, as viewed from above, with a

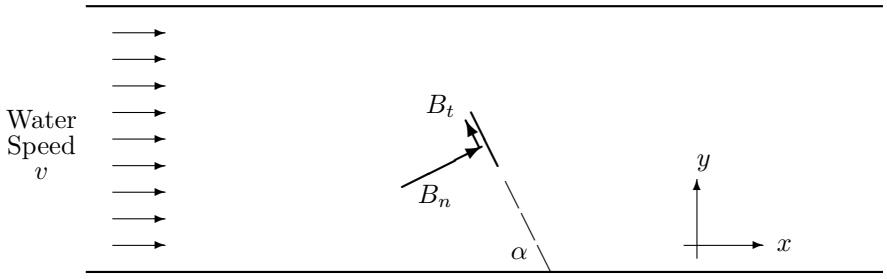

FIG. 2. Schematic view looking down on the experimental arrangement [3], showing the top surface of the water in an open channel. The top edge of the blade can be seen, set level with the water surface. For simplicity the 'blade' shown is the flat plate (with no curvature). Water flows from left to right. The blade face makes an adjustable angle α to the water velocity (or x-axis).

flat blade mounted in the rig. Water flows in an open channel at a measurable velocity. A model blade was attached to a model oar shaft inclined at 10° to the water surface. The blades were aligned 'with the top edge of the blade flush with the water surface' ([3], p. 646). Rowers are generally coached to keep the top edge of the Big Blade level with the water surface during the power stroke, so this is a realistic arrangement for the scale models.[4]

The forces required to hold the blade stationary were measured. The orientation of the blade with respect to the oncoming water, the 'angle of attack' or 'angle

[3]The term 'lift' comes from aeronautical practice. For the blade, the forces act in the horizontal plane, not the vertical plane, but the analogous 'lift' direction is normal to the blade velocity, not the blade chord-line, so Edwards' terminological is not rigorous.

[4]Neither the Macon blade or Big Blade has a straight top edge which could be 'flush with the water surface' along its entire length; it seems clear from Figure 4 in [3] that the Big Blade would be mounted in a realistic orientation with respect to the water level, but it is not clear exactly how the Macon blade is orientated in the tests.

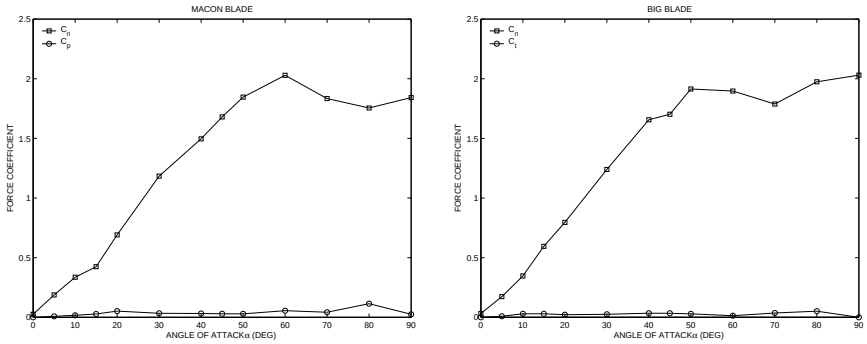

(a) Macon (b) Big Blade

FIG. 3. Normal C_n and parallel C_t force coefficients, from the data in Table 1 of Appendix A.1, and Eqs. 1 and 2.

of incidence' α, could be varied. The components of force parallel/'tangential', (B_t) and normal (B_n) to the chord-line were detected from the bending strains in the supports which held the blade. Caplan and Gardner converted their measured forces to force components parallel to the water velocity F_x and the force component transverse to this direction F_y (across the channel). These are the drag and the so-called 'lift' components of the force. These can be expressed as force coefficients

$$C_D \equiv \frac{F_x}{\frac{1}{2}\rho_w v^2 A_b}$$
$$C_L \equiv \frac{F_y}{\frac{1}{2}\rho_w v^2 A_b}$$

where A_b is the face area of the blade, v is the water velocity relative to the blade and ρ_w is the density of water. The force coefficients, C_D and C_L, scaled from the figures presented by Caplan and Gardner for various blades are given in Appendix A.1.

The force components in the normal and parallel/tangential directions (the forces B_n and B_t) can be expressed as normal and parallel/tangential force coefficients C_n and C_t. These can be derived from the values of C_D and C_L as

$$C_n \equiv \frac{B_n}{\frac{1}{2}\rho_w v^2 A_b} = C_D \sin\alpha + C_L \cos\alpha \quad (1)$$
$$C_t \equiv \frac{B_t}{\frac{1}{2}\rho_w v^2 A_b} = -C_D \cos\alpha + C_L \sin\alpha. \quad (2)$$

The values of C_n and C_t for the Macon blade and the curved Big Blade are shown in Figure 3. For reasons that are explained latter, results are shown for angles of incidence α less than 90° only.

3.1. Estimated friction force

The water friction force along the blade surface would be expected to produce a negative value of C_t. The Reynolds number for the model flow is $\mathrm{Re} \equiv vL_b/\nu$, where $\nu = 1 \times 10^{-6}$ is the kinematic viscosity of water, $L_b = 0.124$ m is the model

TABLE 1
Normal and tangential force coefficients (see Fig. 3), from model tests [3].

α	0	5	10	15	20	30	40	45	50	60	70	80	90
						Big Blade – curved							
C_n	.032	.173	.346	.595	.796	1.24	1.66	1.70	1.91	1.90	1.79	1.97	2.03
C_t	0	.009	.029	.029	.022	.025	.034	.033	.029	.013	.036	.051	0
						Macon – curved							
C_n	.025	.188	.336	.424	.691	1.18	1.50	1.68	1.85	2.03	1.83	1.76	1.84
C_t	0	.008	.017	.027	.052	.034	.032	.030	.028	.057	.042	.114	.025
						'Big Blade' – flat							
C_n	-0.03	.090	.275	.507	.811	1.35	1.74	1.87	1.92	2.03	2.02	1.95	1.86
C_t	0	.002	-0.01	.013	.042	.044	.063	.026	-0.02	.070	.028	.035	0

blade length.[5] The water flow speed is 0.75 m/s. The Reynolds number is

$$\mathrm{Re} \approx \frac{0.75 \times 0.124}{1 \times 10^{-6}} = 90,900.$$

The boundary layer flow over the blade at low angles of attack (when shear/friction is greatest) is likely to be turbulent, and the turbulent assumption gives an upper estimate of the friction forces. The contribution of friction forces to the parallel force coefficient may be estimated as [7] (equation (9.27), p. 410)

$$|C|_{friction} < \frac{0.0594}{\mathrm{Re}^{1/5}} \approx 0.006. \tag{3}$$

The friction force acts on both sides of the blade, so the total contribution to C_t from the friction forces could be as much as 0.012.

3.2. Estimated error in the data

The normal and tangential force coefficients for all three blades (Macon, Big Blade and flat 'Big Blade') tested by Caplan and Gardner [3] are shown Table 1. There are a few results that may indicate the likely margin of error in these force coefficients. The flat Big Blade shows a small negative value of C_n for zero angle of incidence, when the symmetry of the flow requires that $C_n = 0$; that is, when the flat faces of the blade are parallel to the water velocity, the forces normal to the surface should be equal and opposite on the two faces. There is also a maximum positive value of C_t for the flat blade of 0.063 at an angle of incidence of $\alpha = 40°$. Since the pressure forces on the flat parallel sides of the blade have no tangential/parallel component of force, this positive value of C_t, if correct, indicates a difference in the pressures acting on the thin leading and trailing edges of the flat blade. This in turn implies a lower water level at the leading edge than at the trailing edge, leaving part of the leading edge exposed to atmospheric pressure.

We can estimate the maximum *possible* value of C_t by assuming the *entire* leading edge is exposed to the atmosphere. The forward force on the blade results from hydrostatic pressure to a depth D on the trailing edge. This force is $(1/2)\,\rho_w g D^2 t$, where t is the blade thickness and $g = 9.8$ m/s^2 is the standard gravitational

[5] I have estimated values of $L_b = 12.4$ cm and $D = 6.25$ cm for the model. These give $L_b \times D = 77.5$ cm^2, which is approximately equal to the measured area of the flat Big Blade model (77.42 cm^2).

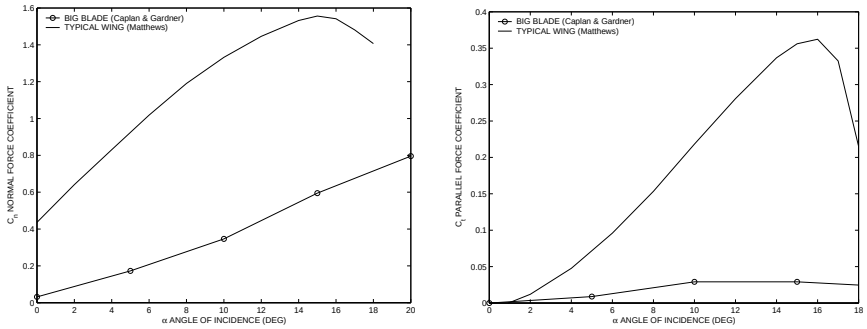

(a) Normal force C_n (b) Parallel (tangential) force C_t

FIG. 4. Force coefficients: Big Blade compared to typical asymmetric wing/airfoil [12].

acceleration at the earth's surface. This force corresponds to a force coefficient of

$$C_t = \frac{\frac{1}{2}\rho_w g D^2 t}{\frac{1}{2}\rho_w v^2 L_b D} = \left(\frac{gD}{v^2}\right)\frac{t}{L_b}. \tag{4}$$

For the (flat) model Big Blade, $t = 0.0018$ m, $L_b \approx 0.124$ m, $D \approx 0.0625$ m and the flow speed v is 0.75 m/s. Thus

$$C_t \approx \frac{9.8 \times 0.0625}{0.75^2} \times \frac{0.0018}{0.124} = 0.016. \tag{5}$$

The reported value of $C_t = 0.063$, though small is significantly larger than this, and may arise from some systematic error in the force measuring system. The difference between the maximum measured value of $C_t = 0.063$ and the expected maximum value $C_t = 0.016$ is 0.047. This suggests that the error in any of the C_t values in Table 1 may be as much as ± 0.05.[6]

4. BLADE AND AIRFOIL COMPARED

The force coefficients for a typical, asymmetrically-shaped 'practical' airfoil/wing are given by Matthews [12]. The difference between the rowing blade (the Big Blade) and the wing can be seen in Figure 4 which shows the normal and parallel force coefficients before the airfoil stalls (at $\alpha \approx 16°$). The airfoil produces normal force coefficients, C_n, which are two or three times larger than those produced by the rowing blade. The airfoil produces parallel force coefficients, C_t, more than ten times larger than those produced by the rowing blade.

The data shows a positive value of the parallel/tangential force coefficient C_t, for all angles of attack, although all the values are less than the possible error of 0.05, and may therefore be zero to within the experimental error. These small positive values of C_t, if reliable, are evidence for the tilt of the blade force which was postulated by Wellicome [14]. The angle of forward tilt of the pressure force is

$$\beta = \tan^{-1}\left(C_t/C_n\right), \tag{6}$$

and Table 2 shows values of β calculated from the data measured by Caplan and Gardner [3]. The values for the Big Blade and the typical airfoil are compared in Figure 5. Note that β for the airfoil force reaches its maximum at an angle

[6] If the front and back surfaces of the model flat blade were not perfectly parallel the pressure forces on these flat faces might have produced this net forward component. Perhaps a similar

TABLE 2
Forward 'tilt' angle $\beta = \tan^{-1}(C_t/C_n)$. C_t and C_n from Table 1.

					'Big Blade' – flat								
α	0	5	10	15	20	30	40	45	50	60	70	80	90
β	0	3.00	-1.31	2.47	1.92	0.50	0.71	0	0.36	0.01	1.49	0.54	0
					Macon – curved								
α	0	5	10	15	20	30	40	45	50	60	70	80	90
β	0	3.00	2.88	3.69	4.29	1.63	1.22	1.01	0.88	1.57	1.32	3.71	0.8
					Big Blade – curved								
α	0	5	10	15	20	30	40	45	50	60	70	80	90
β	0	3.00	4.80	2.80	1.57	1.16	1.17	1.12	0.87	0.39	1.15	1.49	0

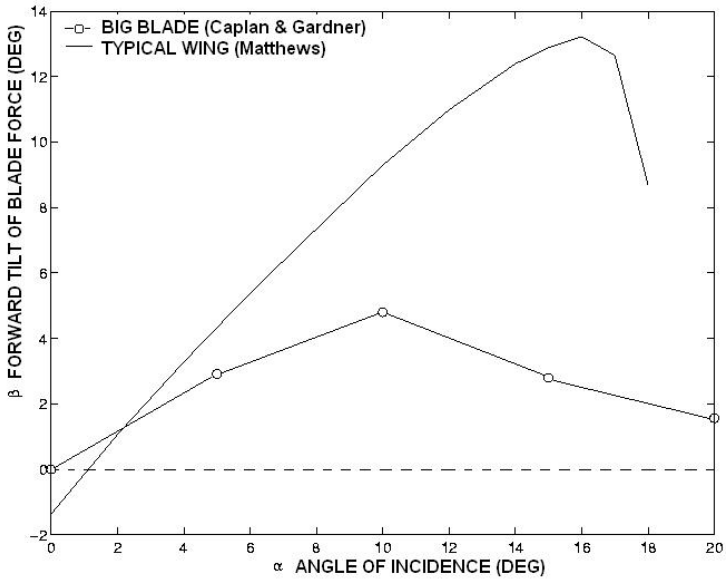

FIG. 5. Forward 'tilt' angle β of blade force compared to that for airfoil force.

of incidence of $\alpha \approx 16°$, after which β decreases as the airfoil stalls. The forward tilt for the blade force, β, reaches its maximum $\alpha \approx 10°$, which suggests that the rowing blade 'stalls' at this angle of incidence.

5. OUTWARD TANGENTIAL FORCE COMPONENT

The forward component of force on an airfoil (*i.e.* the positive value of C_t associated with the forward 'tilt' of the net force) is the result of a non-uniform distribution of pressure forces around the airfoil. The small force coefficients on the rowing blade, compared with the airfoil (see Fig. 4), suggest that there is not a strong analogy between the rowing blade and the airfoil. However, there is a plausible explanation for the positive values of C_t which does not rely on the highly non-uniform distribution of pressure characteristic of the airfoil. The positive tangential force ($C_t > 0$) on the rowing blade could be a result of the asymmetrical

machining error, and similar variation in blade thickness for the curved blades, could produce errors in all the measurements of the amount indicated.

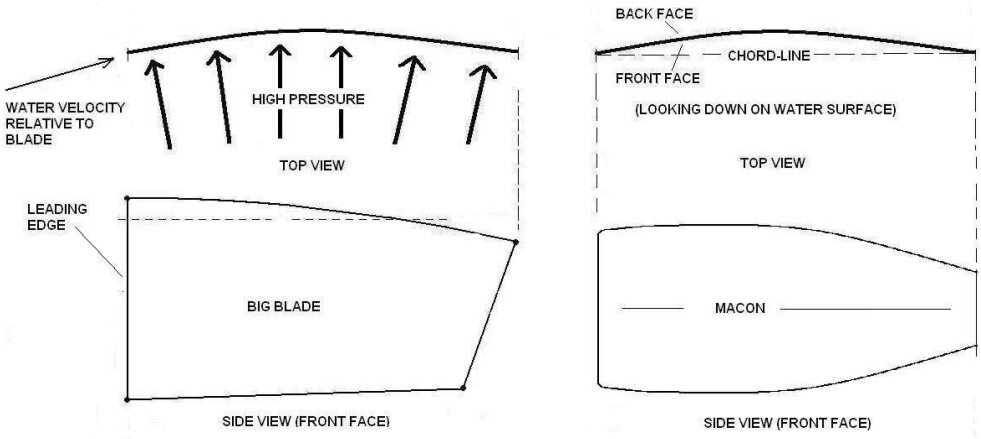

FIG. 6. View of the Big Blade and Macon blade shapes (approximately, and not to scale). The top view shows the blade curvature for either blade, and the water velocity impinging on the front face of the blade. The thick arrows show the net pressure (difference between pressure on the front and back surfaces) acting along the curved blade.

profiles of the Macon and Big Blades; the outward-directed[7] pressures act on a larger area than than the inward-directed pressures.

Sketches of the Macon and Big Blade profile shapes are shown in the side views in Figure 6. The figure also shows a top view (looking down on the water surface and the top edge of the blade) which shows the blade curvature. The water velocity relative to the blade is shown impinging on the front face of the blade.[8] This top view is similar to the top view shown in Figure 2, except that there the curvature of the blade was ignored. In addition the top down view is rotated, with respect to that in Figure 2, which makes the water velocity vector point in a slightly different direction on the page. The top view in Figure 6 shows the pressure acting on the front surface on the Big Blade. Even if this pressure is constant[9], *i.e.* not greater near the leading edge, and even if the lower pressure on the back surface is constant, the net result of these constant pressures will be to produce a component of force acting towards the leading edge if the blade profile is asymmetric, if the area of the blade is greater at the leading edge than the trailing edge.

There is some support for this theory in the measurements made by Caplan and Gardner for two blades having rectangular faces [4], *i.e.* having a constant depth dimension from the leading to the trailing edge. One was curved by the same amount as the model Big Blade, and the other was curved even more. A constant pressure acting on these blades would produce no net parallel force, since the depth at the leading edge is the same as the depth at the trailing edge. Figure 7 shows the measured forward/outwards tilt of the resultant force on these rectangular blades compared with their measurements for the asymmetrical Big Blade [3, 4]. The value for one of the rectangular blades 'switches' between positive and negative values, which suggests, at least, that this data is subject to some experimental error. But even if we assume an error in the values of $\pm 1°$, it seems clear that the forward

[7] 'Outward' means away from the gate or handle of the oar, away from the boat; i.e. a force pointing in the direction from the oar-shaft towards the tip of the oar. This is the positive direction of B_t shown in Fig. 2. Such a force has a forward component relative to the boat direction when the oar is forward of square, but a component backwards when the oar is past square-off.

[8] The front of the blade is the concave 'windward' surface; it faces in the same direction as the rower – towards the back of the boat. The back of the blade is the convex 'leeward' surface which faces to same way as the back of the rower, to the front of the boat.

[9] The model-tests were for steady flow. During rowing the oar is rotating and there might well be a non-uniform pressure distribution along the front face of the blade because of the different speed of each point on the blade relative to the water.

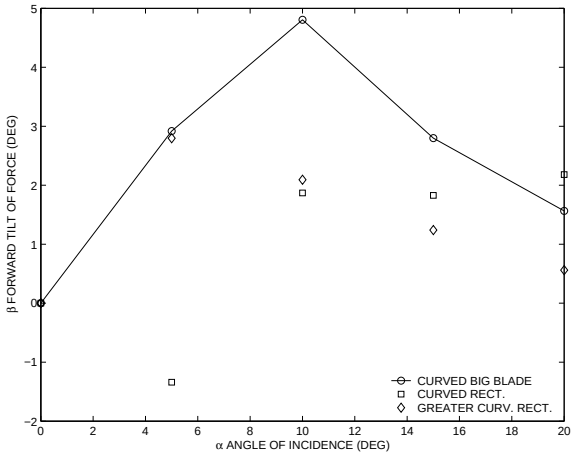

FIG. 7. Forward shift of force direction for curved blades of different profile shape.

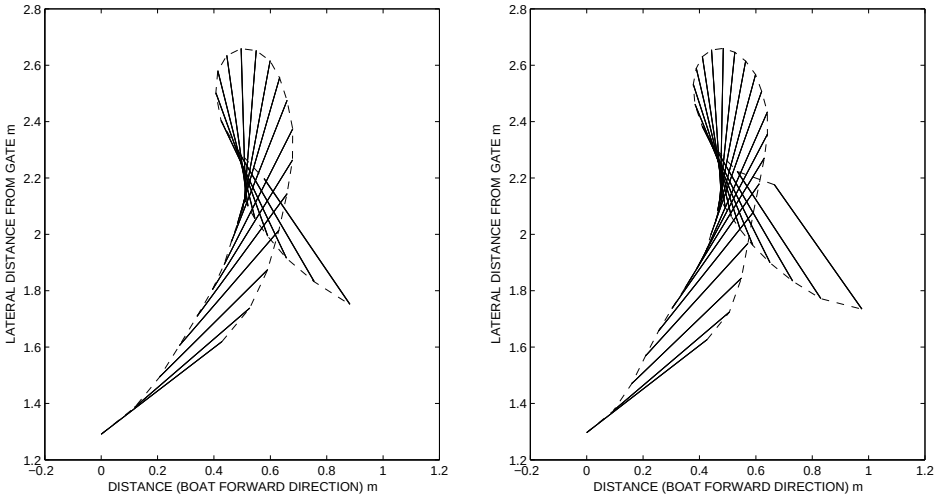

FIG. 8. Path of blade relative to the water. Top view looking down on water. Successive blade positions (chord-line) shown as solid lines. Dashed lines show the paths of the trailing and leading edges of the blade. The boat moves to the right. The oar rotates counter-clockwise.

tilt angle β for the Big Blade, particularly at angles of incidence of $\alpha \approx 10°$, is significantly greater than the tilt angle for the curved rectangular blades, one of which is significantly more curved than the Big Blade. Thus it is more likely that it is the asymmetry of the blade shape that produced this tilt in the force direction, rather than the blade curvature, as would be expected from the airfoil analogy.

6. BLADE VELOCITY RELATIVE TO WATER

A typical path of the blade (relative to the water) is shown in Figure 8 which shows a top view (looking down on the water) of the position of the blade (chord-line) at successive times intervals of 0.043 s, from just after the catch to just before the release for a typical single stroke. The boat is moving to the right and the oar is rotating in the anti-clockwise direction in the horizontal plane.

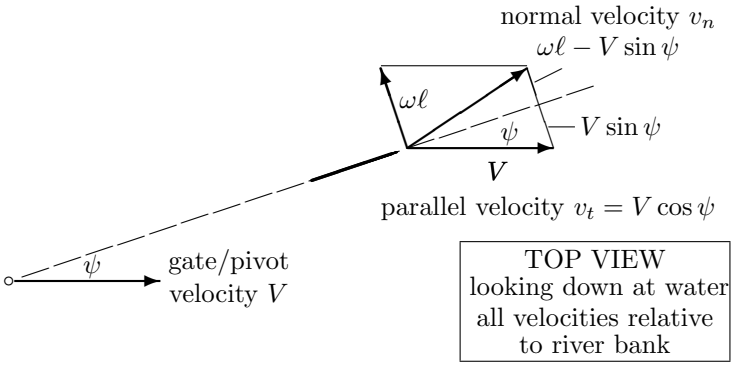

FIG. 9. Components of blade velocity normal and parallel to oar shaft

This figure was constructed from values of measured oar angles, boat speed, and known oar size, supplied by Dr. V. I. Kleshnev[10] who instrumented an eight-oared boat rowed by elite male athletes training at the Australian Institute of Sport. The path of the leading edge, and the path of the trailing edge of the blade are shown as dashed lines. The path of the blade is looped; when the oar is past square-off, it moves through water that it has been disturbed by the blade in the earlier part of the stroke. I have no way of knowing what the blade speed relative to the water is in the latter part of the stroke, because the water through which it is moving has already been set in motion. Since, the angle of attack cannot be known accurately past square-off, the force coefficients measured in the steady flow model tests are of limited value in this part of the stroke. I will confine my analysis of efficiency to the motion of the blade from catch to square-off.

The components of blade velocity relative to the water, during the sweep from catch to square-off, are shown in Figure 9. The components of velocity of one point on the blade, in the directions normal and parallel to the oar-shaft, are

$$v_n = -(\omega\ell - V\sin\psi) \tag{7}$$

$$v_t = V\cos\psi \tag{8}$$

where V is the boat/hull/gate velocity through the water, ψ is the angle the oar-shaft makes to the boat-forward direction, ω is the oar rotational velocity in the horizontal plane and ℓ is the distance from the point on the blade to the gate/pivot. Note that v_n is negative; the positive direction for v_n is the same as the direction of the normal component of blade force B_n. The angle of incidence α, for this one point on the blade, is the angle between the blade chord-line and the velocity of this one point. It is given by

$$\alpha = \tan^{-1}\left(-\frac{v_n}{v_t}\right) = \tan^{-1}\left(\frac{\omega\ell - V\sin\psi}{V\cos\psi}\right). \tag{9}$$

The centre of pressure on the blade, might be approximated as the midpoint of the chord-line, and we could take the value of α for this one point as the 'characteristic

[10]Personal communication, email 16 Feb 2004. Some details of the data-gathering techniques used are given in Ref. [10].

value' for the rotating blade. Similarly, the velocity of the water relative to the blade is different for different points on the blade. This varying angle of incidence and velocity for different points on the blade makes it difficult to use the steady-flow force coefficients to predict the forces developed during rowing. However, we shall see that we do not need to known the magnitude of the force to determine the oar efficiency, but we do need to know, at least, its line of action (direction and 'centre of pressure'). We will take the direction of the force from the relative magnitude of C_n and C_t in the steady flow tests, and we will assume the force acts at the 'centre of area' of the Big Blade, which we have estimated as a distance of $\ell = 2.41$ m (in the horizontal plane) from the gate.

7. EFFICIENCY

The rotational power input to the oar[11] is given by the product of torque applied to the oar and its the rotational speed and can be approximated in terms of the torque of the blade force opposing the rotation as

$$\dot{E}_{in} = B_n \omega \ell \tag{10}$$

where ℓ is the distance of the line of action of the blade force to the gate/pivot, and B_n is the component of the blade force normal to the oar shaft.[12] The power dissipation by the blade is given by

$$\begin{aligned} \dot{E}_{diss} &= -\vec{B} \cdot \vec{v} = -\left(B_n v_n + B_t v_t\right) \\ &= B_n \left(\omega \ell - V \sin\psi\right) - B_t V \cos\psi \\ &= B_n \omega \ell - B_n V \sin\psi - B_t V \cos\psi \end{aligned} \tag{11}$$

where the values of v_n and v_t given in Eqs. 7 and 8 have been used. Note that the boat-forward (propulsive) component of the blade force is

$$B_x = B_n \sin\psi + B_p \cos\psi \tag{12}$$

and that the energy dissipated by the blade can be expressed as

$$\dot{E}_{diss} = B_n \omega \ell - B_x V.$$

This can be expressed by saying the blade dissipates energy (takes energy from the system) by rotating against the blade torque, while at the same time the forward propulsive propulsive force is adding energy to the system at the rate of $B_x V$. The oar efficiency is

$$\eta = \frac{E_{in} - E_{diss}}{E_{in}} \tag{13}$$

$$= \frac{B_n \omega \ell - B_n \omega \ell + B_x V}{B_n \omega \ell}$$

$$= \frac{B_x V}{B_n \omega \ell}. \tag{14}$$

[11] I am ignoring the work done accelerating the rower's mass, which is a form of energy transferred to the hull at a later part of the stroke, particularly during the recovery. This work is important for the overall efficiency of the rowing cycle, but here I am concerned with how much of the rotational energy of the oar, during the drive phase, is converted to linear kinetic energy of the system.

[12] Because of the rotational inertia of the oar, the handle force and blade force are not exactly in phase as the oar first enters the water. See [11] for the equations of motion for the rotating oar.

TABLE 3
Approximate efficiency and propulsive power for first two data points immediately after catch and last two data points immediately before square-off. Force acts at $\ell = 2.41$ m (assumed).

	rate	V (m/s)	ω (/s)	ψ (°)	α(°)	$V\sin\psi/\omega\ell$ %	Power (W)
after	31.8	4.9–4.8	1.75–1.96	40–45	16–22	75–72	299
catch	40.8	5.4–5.2	1.86–2.18	40–43	14–24	77–67	243
before	31.8	5.6–5.7	2.57–2.64	82-88	43–74	90–90	1272
square-off	40.8	6.0–6.2	2.80–2.86	83-88	49–77	88–90	1409

This can be expressed in terms of the force coefficients C_n and C_t as follows

$$\begin{aligned}\eta &= \left(\frac{B_n\sin\psi + B_t\cos\psi}{B_n}\right)\frac{V}{\omega\ell} \\ &= \frac{V\sin\psi}{\omega\ell}\left(1+\frac{C_t}{C_n}\frac{\cos\psi}{\sin\psi}\right). \end{aligned} \tag{15}$$

Equation 14 can also be written in the form used by Wellicome [14]. Let β be the angle between the blade force vector and the direction normal to the oar shaft, so that $B_n = B\cos\beta$. Then the forward propulsive force is $B_x = B\sin(\psi+\beta)$. The efficiency is

$$\eta = \frac{B_x V}{B_n\omega\ell} = \frac{V}{\omega\ell}\frac{\sin(\psi+\beta)}{\cos\beta} \tag{16}$$

8. TYPICAL KINEMATIC VALUES NEAR CATCH AND SQUARE-OFF

Typical values of the hull speed V, oar rotational speed ω and oar angle ψ after the catch and just before square-off ($\psi = 90°$) are shown in Table 3 for two stroke rates. These were derived from the data supplied by Dr. V. I. Kleshnev. The data for each stroke rate consists of a set of 50 equally spaced 'snap-shots' per stroke cycle, each 'snap-shot' being an average over many similar strokes. The table shows values for the first two recorded moments where the blade force B_n is positive (the catch), and the last two moments when for which $\psi < 90°$ (square-off). The values are for an 'average oar', obtained by averaging the oar angles for all 8 oars. The table gives the efficiency calculated by assuming $\beta = 0$ (no forward shift of the blade force), and also the average power $B_n\omega\ell$ which is being supplied by the rower. The efficiency just after the catch (around 75%) is considerably lower than near square off (around 90%) These values are generally consistent with previous studies which have estimated the efficiency of the rowing blade rowing over the entire stroke as follows: 70-75% Affeld *et al.* [1]; 78-85% Kleshnev [9]; 73-85% Hofmijster *et al.* [8]. The efficiencies shown in Table 3 are for high boat speeds (which tend to increase the blade efficiency, according to Eq. 16) whereas the values from the previous studies were for a range of boat speeds.

9. OAR BENDING

The approximate efficiencies shown in Table 3 were derived by assuming that the direction of the blade chord-line is the same as the direction of the oar-shaft axis at the gate where the oar angle was measured. However, because the out-board portion of the oar-shaft oar bends, the direction of the blade force, even if normal to the blade chord, is not normal to the axis of the oar handle. Figure 10 shows a

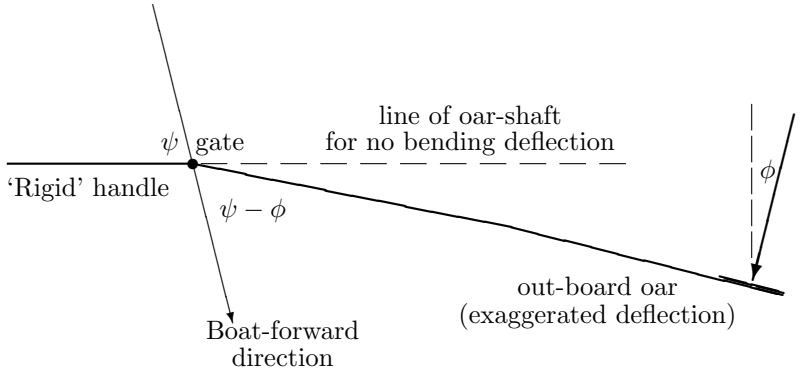

FIG. 10. Schematic of bent oar - exaggerated. The direction of the force changes by angle ϕ because of shaft bending.

top view of the out-board oar, which is bent by the applied force at the blade (in reality the oar shaft deforms into a smooth curved shape, with much less deflection than that shown). For example, when the handle is square to the boat-forward direction, a force normal to the blade chord-line (which is not then square to the boat) has a small component of lateral ('pinching') force, transverse to the boat-forward direction. Brearley and de Mestre [2] included this bending effect in their study of rowing efficiency.

Oar manufacturers express the bending stiffness of an oar by giving the measured deflection under a 10 kg (98 N) load applied at 2.05 m from the gate. Oars of low, medium and high stiffness are produced. For the medium stiffness oar, one manufacture quotes a deflection of 39.5 mm and another 45.5 mm, with an uncertainty of about $\pm$ 6% in each case.[13] For a cantilever of uniform cross-section the angular deflection under a point load is $\phi = 1.5\delta/\ell$ where δ is the deflection and ℓ is the distance of the load from the support. I will assume this relation is accurate enough to relate the angular displacement to the measured deflection for the oars, even though the oar cross-section is not uniform along its length. Taking a typical value of δ as 42 mm we have $\phi = 1.5 \times 0.042/2.05 = 0.03$ (radians) or 1.7° of deflection for the 10 kg (98 N) load, giving an angular bending stiffness of $k = 98/1.7 = 57$ (N/°).[14] The maximum blade force for the average oar (derived from Kleshnev's data) is 305 N (at 40.8 strokes/min) for which $\phi = 305/48.8 = 5.3°$; in the terminology of Brearley and de Mestre, the blade 'lags' the handle by up to 5.3°.

As can be seen in Figure 10, when the handle makes the angle ψ to the boat keel, and the force is normal to the blade, the outboard section of the bent oar is approximately equivalent to the rigid oar, at an angle of $\psi - \phi$ to the forward direction. Hence the efficiency is given by replacing ψ with $\psi - \phi$ in Eq. 16, to get

$$\eta = \frac{V}{\omega\ell} \sin(\psi - \phi) . \tag{17}$$

To get this result I have assumed $\beta = 0$ (*i.e.* assumed that there is no hydrodynamic shift of the force direction). Since any hydrodynamic effect would counteract the effect of oar bending, Eq. 17 gives a lower estimate of the efficiency when the oar

[13] www.bracasportusa.com/products/braca_sharp.htm
www.concept2.com/us/products/oars/sculls/shaft.asp

[14] The stiffness of 57 (N/°) is greater than the stiffness assumed by Brearley and de Mestre. Their maximum blade force was 334.6 N (see their Table 1). The corresponding angular deflection was 7° which gives $k = 334.6/7 \approx 47.8$ N/°. Their maximum blade force is greater than that for the 'average oar' (305 N) but not greater than the most powerful oar (378 N) in Kleshnev's data. The stroke rates differ, 28 strokes/minue [2] and 40.8 strokes/minute (Kleshnev), and their data is for one oar in a men's coxless pair, while Kleshnev's is for all oars in a men's eight.

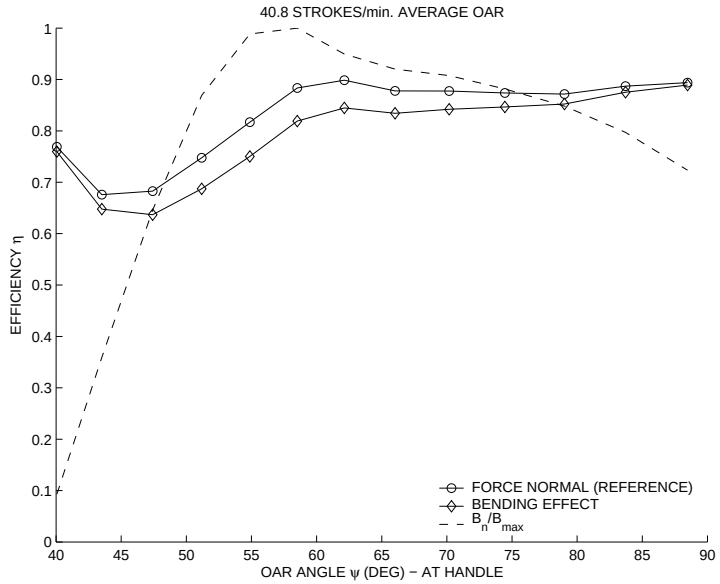

FIG. 11. Efficiency with and without oar-shaft bending. The average efficiency over the sweep shown drops from $\bar{\eta} = 0.83$ (for no bending) to $\bar{\eta} = 0.79$ (due to bending). The broken line shows the blade force as a fraction of its maximum value.

bends. We can use the measured forces to calculate ϕ during the stroke, and use Eq. 17, to calculate the efficiency. We can compare this efficiency for an 'ideal' unbending oar, with no hydrodynamic effect, which can be calculated by putting $\phi = 0$ in Eq. 17. Figure 11 compares the efficiencies in the two cases from catch to square-off. The data shows that bending decreases the average efficiency over the sweep up to square off by some 4% ($\bar{\eta} = 0.83$ compared to $\bar{\eta} = 0.79$). Since the force varies over the stroke, the loss of propulsive power may be different from the loss of average efficiency. The instantaneous propulsive power is

$$\dot{E}_{propul} = B_x V = B_n V \sin(\psi - \phi) .$$

The average propulsive power over the sweep shown is 442.6 W for no bending ($\phi = 0$) and 422.6 W with bending. Thus the propulsive power is nearly 5% less than it could be for an unbending oar, which is not negligible. This estimate does not include the energy lost by heating of the oar due to bending (which would decrease the efficiency somewhat) and does not account for the variations of blade force over the stroke as energy is first absorbed by bending the oar and later released as the oar straightens.

10. POSSIBLE HYDRODYNAMIC EFFECT

The forward shift in the direction of the blade force indicated by the steady flow tests of Caplan and Garner may be as much as 3°. If this is so for full-sized oars as rowed, the average efficiency of rowing may be slightly greater than previously estimated; all three studies referred to above [1, 8, 9] assumed the blade force was normal to the oar-shaft direction at the gate, and no bending of the oar-shaft. Here we also assume no bending, but assume that the force acts forward of normal by the angle β shown in Table 2. Figure 12 shows this effect. The curves show the efficiency if there is no forward shift of the blade force $\beta = 0$, and also if β varies as shown in Table 2. The forward tilt of the blade force would improve the average efficiency by one or two percent in the stroke up to square-off. The possible hydrodynamic tilt of the blade force would decrease the efficiency after square-off, but as about two-thirds of the stroke is before square-off there should be a net

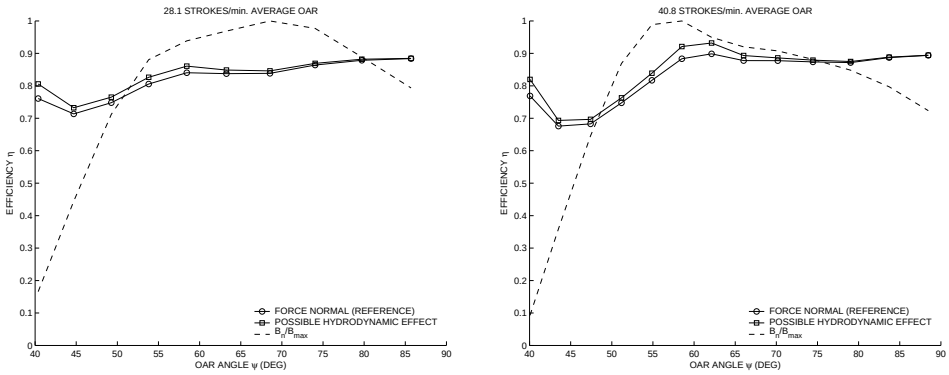

(a) 28.1 strokes/min: $\bar{\eta} = 0.82$ and 0.83 (b) 40.8 strokes/min: $\bar{\eta} = 0.83$ and 0.84

FIG. 12. Efficiency (Eq. 16) for the 'average oar' in a eight, for different oar angle ψ. One curve for $\beta = 0$ (force assumed normal to chord line) and one for forward 'tilt angle' β as suggested by the model tests [3]. No oar bending in both cases. The broken line shows the blade force as a fraction of its maximum value.

increase over the stroke, as was shown by Brearley and de Mestre for a constant 'tilt angle' β over the entire stroke [2].

Figure 12 also shows the variation of the blade force during the stroke up to square-off. The force curve is a rough measure of the available power at each part of the stroke, and the efficiency curve shows how much of that available power is going towards propulsion. For the high stroke rate (40.8 strokes/minute) there *might* be some scope for applying the force/power more effectively. If the peak force was applied somewhat later in the stroke, when the oar angle ψ is greater than 55°, the total power going towards propulsion would be increased, provided *the efficiency curve in the figure remained unchanged*. Of course, the efficiency curve would *not* remain the same if the force were different. The rotational speed of the oar ω would be greater for a greater force and the efficiency would decrease (see Eq. 16) – the blade slips more as the force is increased. A further complication is that the boat speed variation during the stroke would also be changed as the force curve changed, and that also would change the efficiency curves somewhat.

11. CONCLUSION

As shown by Brearly and de Mestre [2], and again here, oar bending has a significant effect (up to 4%) on the efficiency of an oar. It seems clear that rowers should use the stiffest oar they are capable of using comfortably, as is probably well known.

The steady-flow model tests of Caplan and Gardner [3] show a small shift/tilt, forward of normal, in the direction of the blade force on the asymmetrical Macon and Big Blade shapes, *i.e.* there is a small component of force parallel (or tangential) to the blade chord-line, which points in the forward direction. It is possible that this small component of force is actually zero within the experimental error, but if it exists it has important implications for the efficiency of rowing. Previous estimates of the efficiency of rowing have assumed (in the absence of any better data) that the blade force acts in a direction normal to the chord-line. If the direction of the blade force is tilted forward by the amount apparently shown in the steady flow model tests, the efficiency of rowing propulsion may be one or two percent greater than previously estimated. However, these earlier estimates ignored oar-bending and it is possible the opposite errors arising from ignoring oar bending and the possible outwards tilt of the blade force cancel each other.

As mentioned in Appendix A.3, there are reasons to suspect that the scale model results cannot be used to predict the magnitude or the direction of the force on a full-size oar during rowing: the flow is unsteady, but more importantly a crucial non-dimensional parameter, the Froude number, is significantly different in the two cases. The difference between the finite Froude number for a blade being rowed, and the zero Froude number for the hydrofoil/airfoil of hydrodynamic theory means that the blade when rowed cannot generate the large forces generated by ideal, or even practical airfoils operating in the atmosphere. Nor does it seem likely that any significant forward component of force parallel to the blade chord-line is generated by the same mechanism as for airfoils (the change in pressure distribution generated by circulation in the flow). Such a forward force component could be generated by the asymmetrical shape of the blade face for a uniform (chord-wise) pressure distribution. When the curved leading edge is deeper (wider) than the curved trailing edge even a uniform pressure distribution (a high pressure in the water caught in the concave 'spoon') could produce a net forward component of force, parallel to the chord-line. Others have measured the forces acting on an oar during rowing, usually by detecting the bending strains in the oar shaft [1, 8, 9, 10]. These measurements can only detect the components of force normal to the oar shaft. As mentioned in Appendix A.4, it might be possible to detect a component of the blade force, forward of normal, by measuring the tension strain such a force would produce in the oar-shaft outboard of the gate/pivot.

REFERENCES

1. K. Affeld, K. Schichl, and A. Ziemann. Assessment of rowing efficiency. *Int. J. Sports Med.*, 14:S39–S41, 1993.
2. M. N. Brearley and N. J. de Mestre. Improving the efficiency of racing shell oars. *Mathematical Gazette*, 84:405–414, 2000.
3. N. Caplan and T. N. Gardner. A fluid dynamic investigation of the Big Blade and Macon oar blade designs in rowing propulsion. *J. Sports Science*, 25:643–650, 2007.
4. N. Caplan and T. N. Gardner. Optimization of oar blade design for improved performance in rowing. *J. Sports Science*, 25:1471–1478, 2007.
5. Durham Boat Company. Latest development in Dreher oars and sculls, the Apex blade design. www.durhamboat.com/blade_4.php, accessed 22 Nov, 2007.
6. H. R. A. Edwards. *The way of a man with a blade.* Routledge and Kegan Paul, London, 1963.
7. R. W. Fox and A. T. Macdonald. *Introduction to fluid mechanics, 4th ed.* Wiley, New York, 1994.
8. M. J. Hofmijster, E. H. J. Landman, R. M. Smith, and A. J. K. Van Soest. Effect of stroke rate on the distribution of net mechanical power in rowing. *J. Sports Science*, 25:403–411, 2007.
9. V. I. Kleshnev. Propulsive efficiency of rowing. In R. H. Sauders and B. J. Gibson, editors, *Proceedings of the XVII International Symposium on Biomechanics in Sport*, pages 224–228, Perth, Western Australia, 1999. Edith Cowen University.
10. V. I. Kleshnev. Technology for technique improvement. In V. Nolte, editor, *Rowing Faster*, chapter 18. Human Kinetics Inc., 2005.
11. M. N. Macrossan and N. W. Macrossan. Back-splash in rowing shell propulsion. Mechanical Engineering Report 2006/07, espace.library.uq.edu.au/view/UQ:8277, University of Queensland, Australia 4072, 2006.
12. C. Matthews. *Aeronautical Engineer's Data Book.* Butterworth-Heinemann, Oxford, 2002.
13. V. Nolte. Do you need hatchets to chop your water? *American Rowing*, July/August 1993.
14. J. F. Wellicome. Some hydrodynamic aspects of rowing. In J. G. P. Williams and A. C. Scott, editors, *Rowing: A Scientific Approach, A Symposium*, chapter 2. Kaye & Ward Ltd, London, 1967.

APPENDIX: SCALE MODEL AND REAL ROWING FORCES

A.1. SCALE MODEL DATA: STEADY FLOW

Force coefficients scaled from figures given by Caplan and Gardner [3, 4] are shown in Tables 1 and 2. No error bars are shown on the original figures.

TABLE 1

Lift (L) and drag (D) *vs.* angle of attack α.

'Big Blade' – flat ([3] Fig. 6).

α	0	5	10	15	20	30	40	45	50	60	70	80	90
L	-.03	.090	.269	.493	.776	1.19	1.37	1.34	1.22	1.07	.716	.373	0
D	0	.006	.059	.119	.238	.639	1.07	1.31	1.48	1.72	1.89	1.92	1.86

Macon – curved ([3] Fig. 8).

α	0	5	10	15	20	30	40	45	50	60	70	80	90
L	.025	.188	.333	.417	.667	1.04	1.17	1.21	1.21	1.06	.667	.417	.025
D	0	.008	.042	.083	.188	.563	.938	1.17	1.40	1.72	1.71	1.71	1.84

Big Blade – curved ([4] Fig. 7).

α	0	5	10	15	20	30	40	45	50	60	70	80	90
L	.032	.173	.346	.582	.755	1.09	1.29	1.23	1.25	.960	.465	.393	0
D	0	.006	.032	.126	.252	.598	1.04	1.18	1.45	1.62	1.65	1.95	2.03

TABLE 2

Lift (L) and drag (D) coefficients for rectangular blades.

Rectangular – flat ([4] Fig. 5).

α	0	5	10	15	20	30	40	45	50	60	70	80	90
L	-.032	.096	.257	.514	.787	1.20	1.37	1.35	1.22	1.06	.707	.321	0
D	0	0	.032	.096	.257	.659	1.11	1.29	1.40	1.78	1.93	1.99	1.98

Rectangular – low curvature ([4] Fig. 7).

α	0	5	10	15	20	30	40	45	50	60	70	80	90
L	.173	.283	.551	.740	.881	1.31	1.51	1.38	1.38	1.09	.755	.378	0
D	0	.032	.079	.173	.283	.740	1.24	1.38	1.62	1.87	1.95	1.95	2.01

Rectangular – high curvature ([4] Fig. 8).

α	0	5	10	15	20	30	40	45	50	60	70	80	90
L	.191	.413	.571	.778	1.108	1.43	1.57	1.41	1.33	1.11	.762	.381	.064
D	0	.016	.079	.191	.381	.810	1.27	1.44	1.52	1.78	1.92	1.90	1.86

A.2. FULL SIZE OARS: REYNOLDS NUMBER

There are at least two reasons why the force coefficients on the full-size oar blade used in rowing could be different from those in the model tests:

1. an important scaling parameter, the Froude number, is not the same between the model and full-size flow, and
2. the model test measures forces for steady flow, whereas the real flow around the blade during rowing is unsteady.

The general theory of scaling between model tests and full-sized geometrically similar flows (the theory of dimensional analysis) shows that the force coefficients (C_n and C_t), measured on the full-size blades as well as the scale model blades should each be a unique function of the angle of attack α, Reynolds number

$$\mathrm{Re} \equiv vL_b/\nu$$

and Froude number

$$\mathrm{Fr} \equiv v/\sqrt{gD}.$$

I am assuming that surface tension effects are negligible. Here g is the intensity of the gravitational field (acceleration due to gravity) and D is the depth to which the blade is immersed. We expect therefore that the model and full-size data can be represented by unique functions

$$C_n = f_1(\alpha, \mathrm{Fr}, \mathrm{Re}) \text{ and } C_t = f_2(\alpha, \mathrm{Fr}, \mathrm{Re}),$$

The Reynolds number for the full-size flow changes continually through the stroke, and depends on the boat speed. For the full-size flows around real blades being rowed, the Reynolds number varies from $1,500,000$ to $2,000,000$. Although these are twenty times larger than for the model flow, this is probably not significant. As long as the flow is turbulent in the model tests (which seems likely) the normal expectation is that this change in Reynolds number would not alter the flow characteristics significantly. As an example, the friction coefficient (on one side of the blade) for low angles of attack would be 0.004 (see Eq. 3) for the full size oars, as compared with the 0.006 for the model tests. However, in both cases this is negligible compared to the normal force coefficient which may be as large as 2, and the 'Reynolds number effect' on the friction on the blade is negligible.

A.3. EFFECT OF FROUDE NUMBER

The Froude number is important in 'free-surface' flows such as this. For example, the inverse square of the Froude number, gD/v^2, appeared in our estimate of the maximum possible tangential force coefficient on the flat blade (Eq. 4). The square of the Froude number is a measure of the importance of dynamic pressure compared with the hydrostatic pressure near the free-surface (the air-water interface) where the rowing blade operates. The typical hydrostatic pressure within the flow is proportional to $\rho_w gD$ and the expected dynamic pressure (or flow 'momentum pressure') is approximately $\rho_w v^2$. The ratio of these two pressures (which 'drive' the flow) is

$$\frac{\rho_w v^2}{\rho_w gD} = \frac{v^2}{gD} \equiv \mathrm{Fr}^2.$$

For the model flow the Froude number is constant at 0.958. For the flow around the full-size blade the Froude number ranges from about 2.7 at the catch to 0.48 or less at square-off.

The rowing blade operates at the air/water interface where a constant pressure (atmospheric pressure) is applied. The importance of this boundary condition, and its relation to the Froude number, can be illustrated by estimating the lowest pressure that can be developed on the back surface of the blade. As the water speed increases, the pressure will drop and the water level will be lowered. As the water level is lowered, part of the surface of the blade is exposed to the atmosphere, where the minimum pressure (atmospheric pressure P_{atm}) in the flow is established. Any increase in the flow speed can lower the water level even further but it will not decrease the pressure on the already exposed portion of the blade.

For example, consider the flow past the blade in the horizontal plane at a depth $D/2$ below the water level, where D is the depth dimension of the blade. The freestream pressure in this plane is $P_\infty = P_{\mathrm{atm}} + \rho gD/2$. The limiting low pressure on the back of the blade in this plane, is P_{atm} which occurs when the back surface of the blade is exposed to the atmosphere. This limiting low pressure corresponds

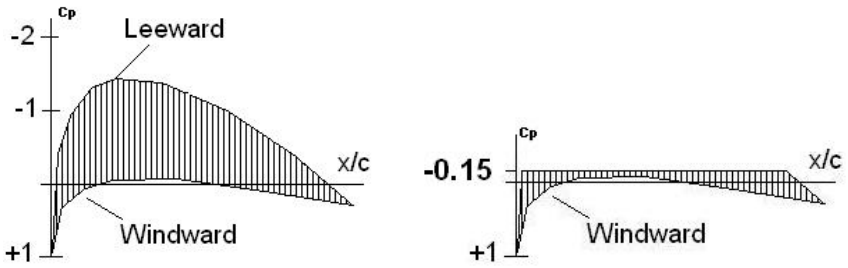

(a) Pressure on airfoil (b) Truncated pressure distribution

FIG. 1. (a) A typical pressure distribution on a airfoil at a small angle of attack. x/c is the fractional distance along the chord from leading to trailing edge. The windward (lower) surface pressure and leeward (upper) surface pressure is shown for each location x/c. $C_P \equiv 2\left(P - P_\infty\right)/\rho v_\infty^2$ is the pressure coefficient. P_∞ is the static pressure and v_∞ is the flow speed, far upstream. (b) The same pressure distribution truncated at $C_P = 1/\mathrm{Fr}^2 = -0.015$. The total force is proportional to the shaded area in both cases.

to a limiting pressure coefficient of

$$C_P \equiv \frac{P - P_\infty}{\frac{1}{2}\rho v^2} = \frac{P_{\mathrm{atm}} - (P_{\mathrm{atm}} + \rho g D/2)}{\rho v^2/2} = \frac{-gD}{v^2} = -1/\mathrm{Fr}^2$$

The depth dimension of the blade, D, is approximately 0.250 m and the freestream water speed relative to the blade is approximately 4 m/s at the catch (for 40.8 strokes/min). The Froude number is

$$\mathrm{Fr}_{\mathrm{blade}} \approx \frac{4}{\sqrt{9.8 \times 0.25}} \approx 2.6$$

and the minimum pressure coefficient coefficient is

$$C_P = -1/2.6^2 \approx -0.15.$$

A typical pressure distribution around an airfoil/hydrofoil at a low angle of attack is shown in Figure 1(a). There are very low pressures on the upper (leeward) surface and the difference between the pressures on the lower (windward) surface and these low pressures on the upper surface produce the large net forces characteristic of an airfoil. Because of the limiting value of C_P, we cannot establish this 'airfoil-like' pressure distribution on a rowing blade; if we wanted to estimate the pressure distribution on the blade with the help of the airfoil analogy, we would have to assume a distribution something like the truncated distribution shown in Figure 1(b), for which the net force is much reduced.

For subsonic flight of an airplane wing at typical altitudes the Froude number effect can be shown to be negligible. Even for a high (but subsonic) flight speed of $v = 500$ km/h (139 m/s) the dynamic pressure is $\rho_a v^2/2 = 1.2 \times 139^2 \approx 12$ kPa, which is small compared to the freestream (atmospheric) pressure of approximately 100 kPa. For the limiting zero pressure on the airfoil, the pressure coefficient is

$$C_P = \frac{0 - P_{\mathrm{atm}}}{\frac{1}{2}\rho_a v_\infty^2} = \frac{-100}{12} = -8.3.$$

The minimum values of $C_p \approx -1.5$, seen in the pressure distribution for an aerofoil, is not close to this limiting value. The equivalent depth of immersion of the airfoil in the atmosphere (assuming constant air density) is $D = P_{\mathrm{atm}}/\left(\rho_a g\right) \approx 8,500$ m.

The characteristic speed is $v_c = \sqrt{gD} \approx 288$ m/s, and the Froude number is

$$\mathrm{Fr}_{\mathrm{flight}} = \frac{v}{v_c} = \frac{139}{288} = 0.49.$$

For higher subsonic flight speeds, approaching v_c, the Froude number will become important, but in that case, the effects of compressibility of air make the standard hydrodynamic theory of the airfoil invalid.[15]

The Froude number for the model-tests, of 0.985, is closer to the low values typical of practical airfoils in the atmosphere, than is the Froude number for the full-size rowing blade at the catch (≈ 2.6). The force coefficients for the model-tests were significantly smaller than for an airfoil, and it should be expected that the even larger Froude number for the full-sized blade would make the the rowing blade even more unlike an airfoil.

A.4. FULL-SIZE OARS: UNSTEADY FLOW

The two data points at the catch (for the stroke rate of 40.8/muinute), which were shown in Table 3 in §8, were separated by only 0.014 s. During this time the angle of incidence α changed from 14° to 24°, while the oar swept from $\psi = 40°$ to $\psi = 43°$. During this time, the water flowing past the blade (from Kleshnev's data I calculate a blade speed relative to the water at the catch of 4 m/s, for the 40.8/min stroke rate) has travelled only $4 \times 0.014 = 0.056$ m which is only slightly more that 1/10 of the distance from the leading to trailing edge of the blade. It hardly seems likely that anything like a quasi-steady flow can be established when the angle of incidence changes by 10° before the fluid has travelled such a small distance along the blade.

At zero angle of attack, for both blades, the scale tests show a small lift coefficient (and zero drag coefficient). This might be achieved in practice if, at the first entry of the oar into the water, the blade velocity relative to the water is parallel to the oar shaft. This 'perfect' entry requires that the oar be rowed through the air by a small amount, such that at the moment of first contact with the water $\omega\ell = V \sin\psi$ so that α in Eq. 9 is equal to zero. Only one point on the oar-blade (one value of ℓ) can have the velocity required to meet this condition. The tip may enter the water at zero angle of attack so that a small 'pure lift' is generated, which would be 100% efficient (dissipating no energy). But this force cannot be significant to the overcall propulsion system; it is small because C_n is small, and only a small fraction of blade area is immersed, and it cannot last for long because the continued rotation of the oar quickly increases the angle of attack.

If the blade force is titled significantly forward of normal there would be a tension strain in the oar shaft *out-board of the gate*. This tension could be detected with strain gauges attached to the out-board portion of the oar shaft. It would be helpful to know the variation of water level on both sides of the blade. The Durham Boat Company [5] has used a small camera attached to an oar being rowed, to view the water flow around the blade. An oar equipped with a similar camera and out-board strain gauges would provide the sort of information required to better understand the flow around a moving oar blade.

[15]The critical speed is $v_c = \sqrt{gD} = \sqrt{P_{\mathrm{atm}}/\rho_a} = \sqrt{RT_a} = 288$ m/s, where $P_{\mathrm{atm}} = \rho_a R T_a$. Here $R = 287$ J kg^{-1} K^{-1} is the gas constant for air, and T_a is the atmospheric temperature. The speed of sound in air is $a = \sqrt{1.4RT_a} \approx 347$ m/s, close to the critical speed v_c, so the Froude number is approximately the same as the Mach number.